Supporting Information

Molecular Dynamics Pinpoint the Global Fluorine Effect in Balanoids Binding to PKCε and PKA

*Ari Hardianto, Fei Liu, Shoba Ranganathan**

Department of Chemistry & Biomolecular Sciences, Macquarie University, Sydney, NSW 2109, Australia

(*Email: shoba.ranganathan@mq.edu.au)

Note 1 Stereoelectronic effects of fluorine

Unlike other halogens such as chlorine and bromine, fluorine is a small atom with size of 1.47 Å which is closer to 1.20 Å for hydrogen (**Table S1**). Therefore, substituting hydrogen atom to fluorine does not significantly increase the size of an organic molecule. Fluorine forms a highly polarised C–F bond which is significantly stronger than C–H, C-Cl and C-Br bonds, since it is the most electronegative element with Pauling electronegativity of 4.00 (Table S1), compared to other halogens. The attraction of partial positive and partial negative charges on carbon and fluorine atoms, respectively, makes the C-F bond short and strong with significant ionic character. Additionally, C-F bond has three lone electron pairs on the fluorine which is quite unreactive[1.1] As a result of its unique characters, the C–F bond convey a perturbation that can changes the conformation of a ligand molecule. This fluorine perturbation is provided by conformational effects of the C-F bond including: dipole–dipole interactions, charge–dipole interactions, and hyperconjugation effects.[1, 2]

Dipole–dipole interactions

The polarisation of the C-F bond enables participation in dipole-dipole interactions[1.1] The interactions are not only between molecules (intermolecular) but also within a molecule (intramolecular). Examples of intermolecular dipole-dipole interactions are fluorinated drug binding to their receptors with the fluorine atom oriented towards a partial positive charge, such as an amide carbon atom or the hydrogen atom of a hydroxyl group (**Figure S1**.A: **1** and **2**). While these intermolecular dipole-dipole interactions are weak, intramolecular dipole-dipole interactions are stronger. For instance, the conformation preference of α–fluoroamide[2] (Figure S1.A: **3**) in

which the C–F bonds align antiparallel to the C=O bond, is the result of intramolecular dipole-dipole interactions.

Charge–dipole interactions

The partially negative fluorine ($F^{\delta-}$) in the C-F bond can also make a charge-dipole interaction if it is close to a formally positive-charged oxygen or nitrogen atom.[1] Such interactions shape a molecule where the $F^{\delta-}$ is in proximity to the formal positive charge. For example, 2–fluoroethyl ammonium ion (Figure S1.B: **4**), protonated 2–fluoroethanol (**5**) and 2–fluoroethylpyridinium ion (**6**) strongly favour *gauche* conformers due to proximity of $F^{\delta-}$ to N^{+}.

Hyperconjugation effects

Every C-F bond has a vacant low-energy antibonding orbital (σ*) which can participate in hyperconjugation with adjacent C-H bonds.[1] The hyperconjugation effect explains NMR and molecular modelling studies that show the *gauche* conformer of 1,2-difluoroethane is more stable than the *anti*. In the *gauche* conformer, the antibonding orbital of C-F bonds (σ*C-F) are aligned with the neighbouring bonding orbital of C-H bonds (σC-H) and gives a stabilisation effect of hyperconjugation. Hyperconjugation makes the C-F bond longer and less covalent than the C-H bond. Besides 1,2-difluoroethane, the hyperconjugation effect can be found in various systems **(**Figure S1.C: **7**–**11**) such as F–C–C–O and F–C–C–N groups. Moreover, lone pair electrons (Figure S1.C: **12**–**13**)[3, 4] and π–systems[5] also can participate in hyperconjugation with σ*C-F.

Note 2 Interaction of the balanol (1) in the ATP sites of PKA and PKCε

Despite having a fix conformation, the azepane ring of **1** moves gently in the ribose subsite of PKA, as monitored in Figure 2.A. The source of this movement may be from the presence of two hydrogens on the positively charged amine group. Each hydrogen interacts with different residues around ribose subsite. One hydrogen interacts via an H-bond with backbone of Glu171, whereas the other makes an H-bond with side chain of Asp185 (Figure S11; Table S3). Nevertheless, the position and the fix conformation of the azepane ring as well as the corresponding residues in the ribose subsite cannot accommodate both H-bonds at the same time. If one H-bond is formed, it breaks the other H-bond (data not shown). These competitive H-bonds cause a movement on azepane ring (main paper: Figure 2.A) which sways the whole balanol structure upon binding, as indicated by the dihedral plot $\omega 6$ (Figure S7). This movement may distract and reduce the conservation of the H-bond between C5'-OH of benzamide and Glu122. But, the benzamide remains firmly docked due to the presence of an H-bond between the C1'=O of benzamide and Thr184. In addition, interactions contributed by the benzamide aromatic ring and surrounding hydrophobic residues also assists the moiety to settle in the adenine subsite. In the triphosphate subsite, the benzophenone moiety builds interactions through a π-π stacking (ring D of benzophenone and Phe55) and H-bond networks. These H-bonds include interactions of benzophenone with Glu92, Ser54, and Phe55.

In its limited flexibility conformation, the azepane ring of **1** has a mobility in the ATP site of PKCε in which it moves up from the initial pose (main paper: Figure 2.A and C). Despite this mobility, the benzamide moiety retains high H-bond conservation of 84% which is higher than PKA-bound **1** (78%; Table S3). In addition, the benzamide moiety also makes a transient H-bond

with Lys437. The benzophenone moiety intensively interacts with Glu456 (corresponding to Glu92) via C10"-OH, but it is completely lost interaction with Gly-rich loop residues.

Note 3 Interactions of balanoids 1a and 1e in the ATP site of PKCε

As suggested by our previous work,[6] C6(*S*)-fluorinated balanol analogue may present as two species with different charge states in the ATP site of PKCε. One form (**1a.1**) bears a charge only on the carboxylate C15″O_2H group, whereas the other species (**1a.2**) has charges on the amine N1, the phenolic C6″OH, and the carboxylate C15″O_2H groups. Both species exhibit different conformations on their azepane rings as monitored in polar plots of dihedral angles (Figure S8, **1a.1** and **1a.2**). The plots show that **1a.2** undergoes conformation changes from its initial conformation. Also, the fluorine atom in **1a.2** is not able to satisfy a C-F$\cdots N^+$ gauche alignment which is consistent with our previous studies.[7, 8] The azepane rings of both species share similar interactions in the ribose subsite of PKCε. In both charged state species, the fluorine substituent forms intramolecular interactions with the O-ester linkage. Also, the N1 amine interacts with the backbone of Asp536 via an H-bond, where **1a.1** confers conservation of 54%, whereas **1a.2** is 45%. Interestingly, although **1a.1** has a slight unfavourable binding contribution of 0.02 kcal.mol^{-1} with Asp449, both species show similar binding energy contribution with the ATP site residues of PKCε.

In PKCε, fluorine perturbation in **1e** results in a different restrained conformation on its azepane ring compared to that bound to PKA (Figure S7, dihedral angles of **1e**). Such conformation is due to replacement of Thr184 (in PKA) by Ala549 in PKCε. Additionally, substitution of Glu171 to Asp536 in PKCε may also contribute to the azepane ring conformation since Glu has a longer side chain than Asp allowing interaction with fluorine.

The fluorine atom on C5(*S*) of the azepane ring interacts with the side chain of Asp536, whereas Asp550 is with another fluorine on C6. Meanwhile, the uncharged N1 amine group forms H-bonds with the side chains of Asn536 and Asp550. Similar to PKA-bound **1e**, water-mediated intramolecular interactions between C5(*S*)-F and N of the amide linkage also participate in the restraint process. Hyperconjugation also occurs between σC7-H and σ*C6-F2 that may contribute to restraining the azepane ring conformation (Figure S6, **1e** in PKCε). The restrained azepane ring further limits the flexibility of amide and ester linkage (Figure S8, dihedral angle ω_6 of **1e**) that leads to the inability of the azepane ring to accommodate the other moieties to interact better with the ATP site residues. As shown in the Table S3 of H-bond conservation, the benzamide moiety of **1e** is missing H-bonding interactions with the adenine subsite residues, Glu487 and Val489. As a result, the docking of the benzamide moiety is rather pulled away from the adenine subsite of PKCε (main paper: Figure 2.C).

Similarly, despite **1e** considered as a weak PKCε-binder (K_d of 38 nM), it does not exhibit any unfavourable binding interactions in the ATP site of PKCε. Nonetheless, the binding energy of **1e** and some residues at the adenine subsite are weak (Figure S9), reflecting the poor interaction of the benzamide moiety with the residues at this subsite.

Note 4 Hydrogen bond network and binding energy contribution

Among the balanoids considered in this study, interactions of the azepane ring with residues in the adenine subsite of PKA as well as PKCε display similar profiles of binding energy contribution (Figure S9) and hydrogen bond (H-bond) (Table S3). The only exception is **1e** in PKCε, where weaker binding contributions with the loss of some H-bonds occurring with the adenine subsite residues (**Note 2**).

Fluorine substitution on the azepane ring, as expected, alters H-bond interactions between the amine N1 group of balanoids and residues in the ribose subsite (Table S3). In PKA, where most of balanoids show comparable affinities (main paper: Table 1), H-bond network alterations are similar among balanoids. Likewise, binding energy contributions of residues in the ribose subsite to PKA-bound balanoids (Figure S9) are within a narrow range, except for Asp185 (-9.70 kcal.mol^{-1} for **1a.1**). On the other hand, in PKCε, the contributions of residues around the azepane ring are widely dispersed (-0.17 to -5.32 kcal.mol^{-1}). In particular, the contribution of residue Asn537 ranges from weakly repulsive (+0.28 kcal.mol^{-1} for **1d**) to strongly attractive (-8.30 kcal.mol^{-1} for **1a.1** and **1a.2**).

The effect of fluorine perturbations also cascades to the interactions of the benzophenone moiety with residues in the triphosphate subsites. While in PKCε the perturbations have limited effect on the H-bond network with Glu456 (Table S3), in PKA the connections with the corresponding residue Glu92 are either increased or decreased, which is also reflected in the binding energy contribution. In PKCε, fluorine perturbations cause the Gly-rich loop residues (Ser418 and Phe419) to form more extensive H-bond interactions with the benzophenone moiety. However, these contributions appear to be small as the binding energy contribution profiles shown by these residues in PKA and PKCε are similar (Figure S9).

To sum up, fluorine perturbation on the azepane ring affects the interactions of the moiety with the ribose subsite residues and remotely alters the interactions of the benzophenone moiety with the triphosphate subsite. However, fluorine perturbation less interferes the benzamide moiety in the adenine subsite.

Note 5 The limitation of Thr184 in handling tri-fluorine perturbation

In PKA, Thr184 hold the C1'=O in the ester linkage of all balanoids and further restrains their azepane rings. The restrained azepane rings attenuates fluorine perturbations to interfere other moieties, particularly the benzophenone moiety. As a result, most fluorinated balanol analogues do not show considerable binding affinity changes (main paper: Table 1). However, Thr184 in PKA shows a limitation to handle fluorine perturbation in **1e** which causes a decrease binding affinity.

Balanoid **1e** has three fluorine atoms that restrain the azepane ring into a particular conformations using water-mediated intramolecular interactions (Figure S11.F, left panel, highlighted by green halo). This restraint also involves intermolecular interactions, which include the interaction of a fluorine atom on C6 with the side chain of Glu171 and an H-bond between the non-protonated amine N1 and the backbone of the same residue (Figure S11.F, left panel; Table S3). Hyperconjugation between σC7-H and σ*C6-F3 may also participate in stabilising the restrained conformation (Figure S6, **1e** in PKA). The H-bond contributed by Thr184 (Table S3) more restrains the azepane ring and impedes this central moiety to accommodate interactions between the benzophenone moiety and residues in the triphosphate subsite. As a consequence, Glu92 in the triphosphate subsite contributes to unfavourable binding interaction of 0.40 kcal.mol^{-1} (Figure S9) with the benzophenone moiety which may responsible for the decrease affinity of **1e** to PKA.

Table S1 Properties of some halogens in organic compounds compared to hydrogen.[1]

Properties	H	F	Cl	Br
van der Waals radius (Å)	1.20	1.47	1.75	1.85
Pauling electronegativity	2.10	4.00	3.20	2.80
Length of single bond to carbon (Å)	1.09	1.40	1.77	1.97
Strength of bond to carbon (kcal/mol)	98.8	105.4	78.5	66.0
Relative reaction rate for halide ion removal	-	1	71	3500

Table S2 Wilcoxon sum-rank test on RMSF of balanoids-bound PKCε and PKA compared to their *apo* form.

PKCε						
Analogue*	**1**	**1a.1**	**1a.2**	**1c**	**1d**	**1e**
K	1.16×10^{-15}	2.27×10^{-21}	1.38×10^{-16}	1.85×10^{-21}	1.55×10^{-21}	1.68×10^{-9}
G	2.60×10^{-2}	2.16×10^{-3}	2.16×10^{-3}	2.16×10^{-3}	2.16×10^{-3}	2.16×10^{-3}
A	8.00×10^{-5}	7.42×10^{-9}	1.29×10^{-9}	2.30×10^{-8}	2.06×10^{-8}	1.74×10^{-5}
PKA						
Analogue*	**1**	**1a.1**		**1c**	**1d**	**1e**
K	3.32×10^{-14}	4.06×10^{-2}	-	2.16×10^{-15}	7.61×10^{-14}	1.28×10^{-15}
G	2.16×10^{-3}	2.16×10^{-3}	-	2.16×10^{-3}	2.16×10^{-3}	2.16×10^{-3}
A	8.15×10^{-6}	4.05×10^{-2}	-	1.26×10^{-6}	3.59×10^{-5}	6.32×10^{-6}

*K denotes kinase domain, G is Gly-rich loop, and A is ATP site.

Table S3 **H-bond conservation in MD simulations of PKA and PKC**ε. The table lists persistence of H-bond networks between balanoids and the ATP site residues of PKA as well as PKCε.

		PKA							PKCε							
				H-bond conservation (%)							H-bond conservation (%)					
Moeity*		**Residue#**		**1**	**1a.1**	**1c**	**1d**	**1e**	**Residue**		**1**	**1a.1**	**1a.2**	**1c**	**1d**	**1e**
Bp	C15"OOH	Ser54	BB	50	73	61	62	73	Ser418	BB		46	24	17	77	62
Bp	C15"OOH		SC	5	84	11	99	93		SC		70	5	4	100	61
Bp	C8"=O		BB	4												
Bp	C15"OOH	Phe55	BB	4		2			Phe419	BB		1	36	67		14
Bp	C8"=O		BB	29	39	25	21	57		BB		38	7		41	6
Am	C1'=O	Lys73							Lys437	SC	48	20	39			77
Bp	C6"-OH		SC	3	2		17			SC			3	69		
Bp	C10"-OH		SC	6	6	2	3	4								
Bp	C10"-OH	Glu92	SC	85	2	99	98	3	Glu456	SC	100	99	100	98	98	99
Bm	C5'-OH	Glu122	BB	78	87	58	79	81	Glu487	BB	84	88	84	89	68	
Bm	C5'-OH	Val124	BB	15	17	18	9	31	Val489	BB	15	29	19	19	20	
Az	N1	Glu171	BB	29	66	57	49	79	Asp536	BB	38	54	45			
Az	N1	Asn172	SC	24		1		1	Asn537	SC	1			34		25

		PKA							PKCε						
				H-bond conservation (%)							H-bond conservation (%)					
Moeity*		**Residue#**		**1**	**1a.1**	**1c**	**1d**	**1e**	**Residue**		**1**	**1a.1**	**1a.2**	**1c**	**1d**	**1e**
Am	C1'=O	Thr184	SC	46	19	90	80	82	Ala549							
Az	N1	Asp185	SC	22		1	23		Asp550	SC	42		1	66		63
Bp	C6"-OH		SC	1	100	1	1	1		SC		91				
K_d **(nM)**				5.9	7.9	6.4	9.2	43			0.73	19	19	0.4	110	38

*Moieties in balanoids which include Bp or benzophenone, Bm benzamide, and Az azepane, whereas Am denotes amide linkage.

#BB: residue backbone; SC: residue side chain

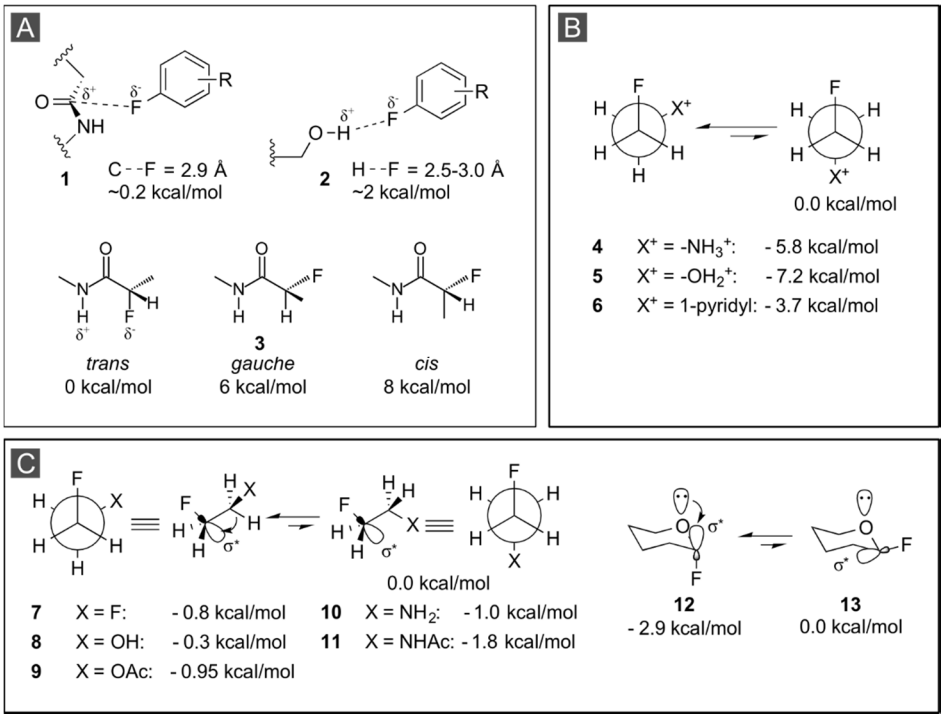

Figure S1 **Conformational effects of fluorine**. (A) dipole–dipole interactions, (B) charge–dipole interactions, (C) hyperconjugation effects. Figures are adapted from Hunter,[1] Gillis *et al*,[2] Juaristi *et al*,[3] Kirsch *et al*,[4] and Tozer and David.[5]

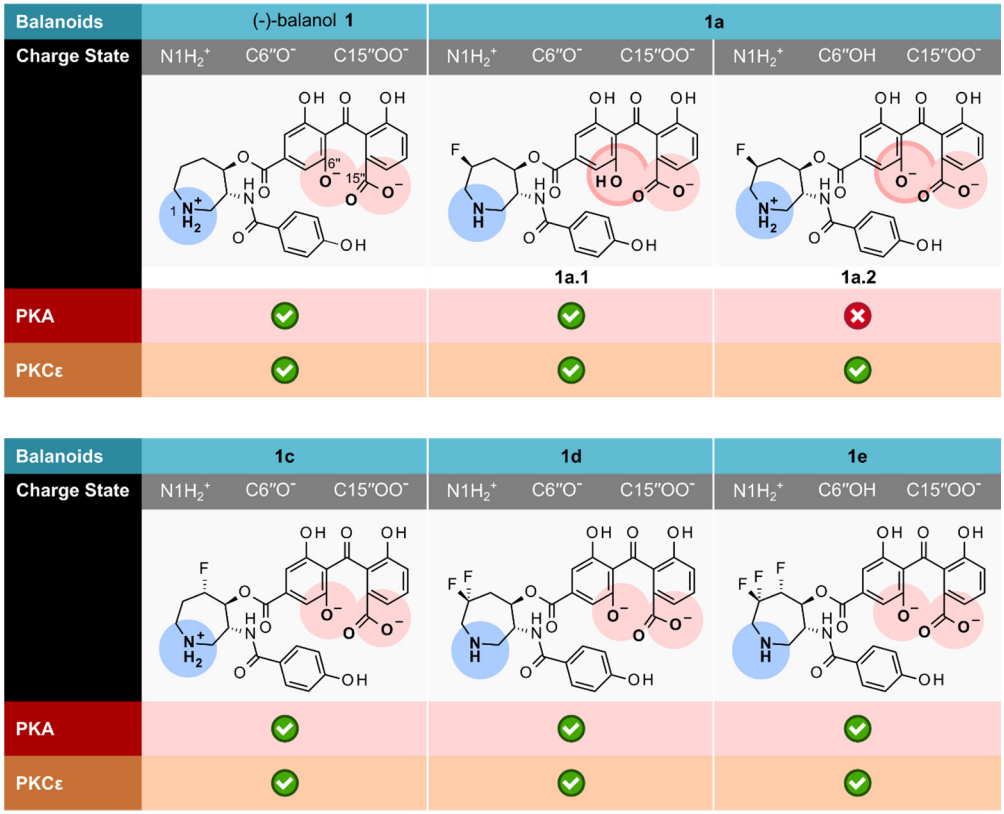

Figure S2. Charge states of balanoids in the ATP sites of PKA as well as PKCε. Under biological assay pH, a positive or negative formal charge possibly appears on the amine N1, and the phenol C6″OH, and the carboxyl C15″OOH. As suggested by a previous study,[6] all balanoids have same charges states in both PKA and PKCε, except **1a**. In PKCε, **1a** presents as two species: **1a**.**1** which only bear a charge on C15″OOH; and **1a**.**2** where charges appear on N1, C6″OH, and C15″OOH. In PKA, only **1a**.**1** exists. . Fluorination of balanol influences the basicity of N1. In the case of **1a**, monofluorination on the carbon β to N1 decreases the basicity of the amine group and turns it unprotonated. Incorporation of one fluorine atom on carbon γ to N1 (**1c**) also reduces the basicity of N1, but the charge state does not alter. Balanoids undergo a more noticeable effect of charge state alteration when di- or trifluorination is introduced in the azepane ring. Additionally, the nature of the ATP site also affects the formal charges of N1 and C6″OH.

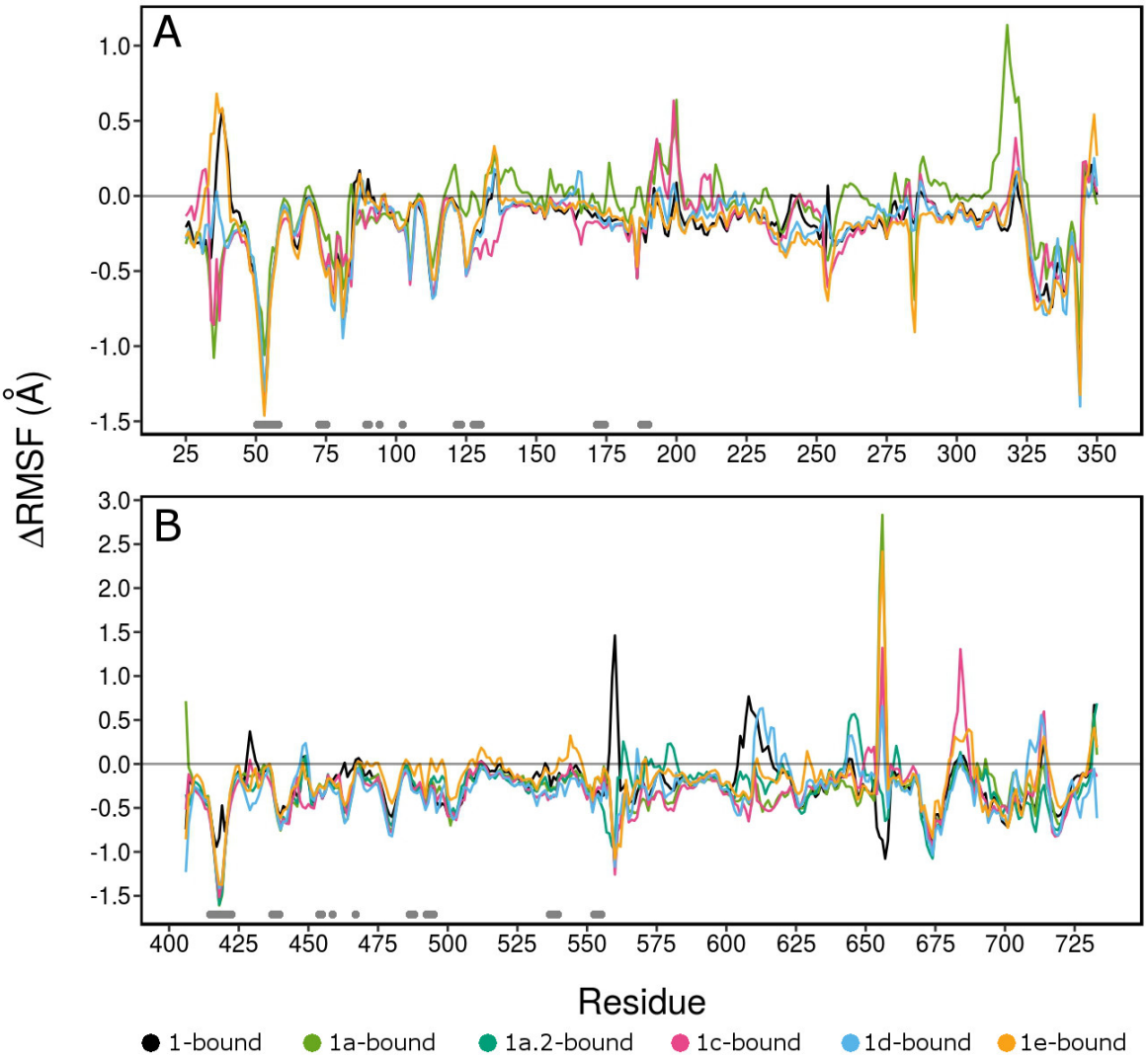

Figure S3. Root-Mean-Square Fluctuation (RMSF) changes of (A) PKA and (B) PKCε following balanoid binding. ATP site residues are indicated by grey bars near the x-axis in each graph.

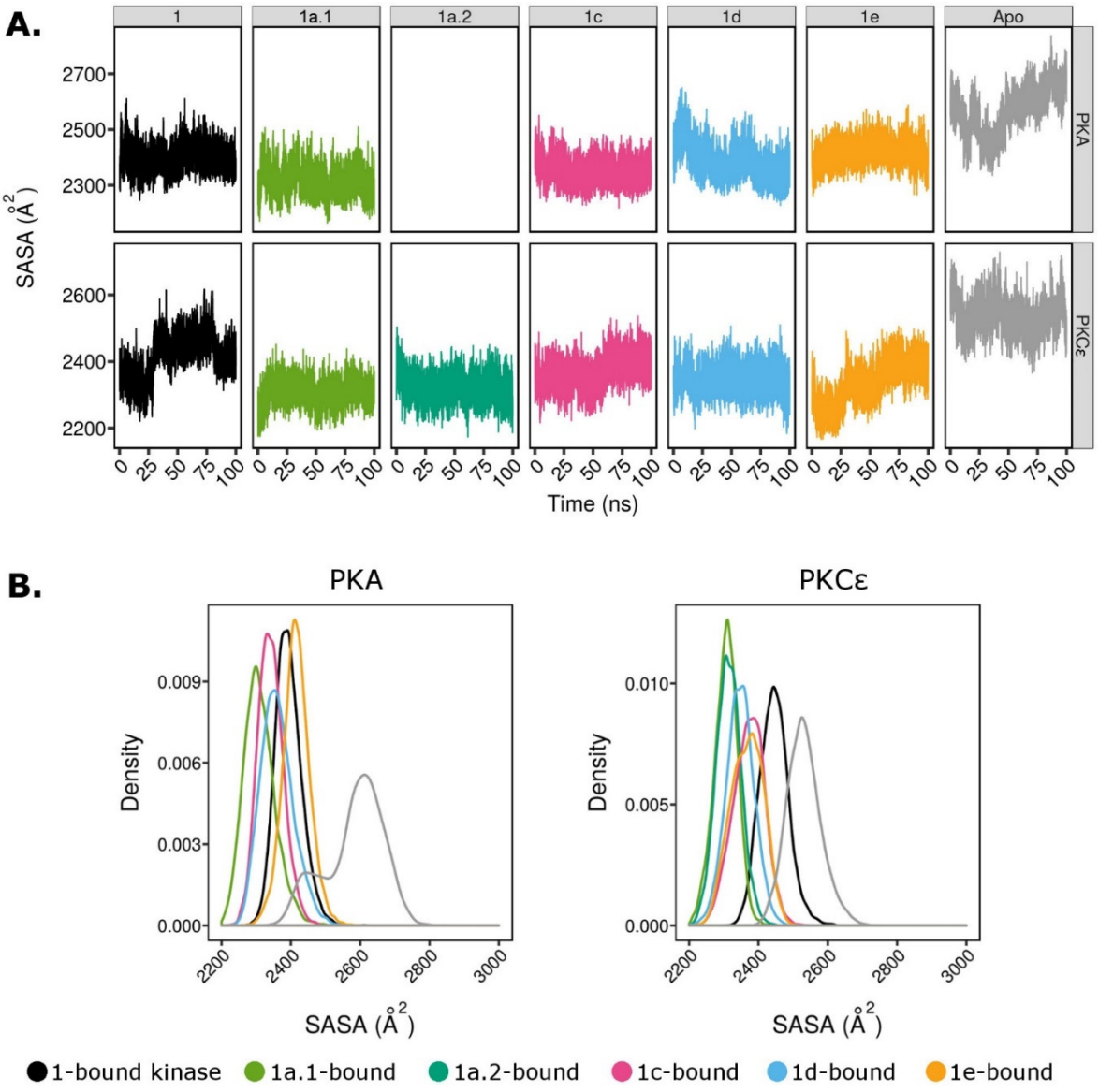

Figure S4 Solvent-Accessible Surface Area (SASA) of balanoid-bound and *apo* forms of PKA and PKCε. (A) SASA is presented in trajectory plots and (B) depicted in density curves. In the case PKCε, **1a.1** represents the C6(S)-fluorinated analogue carrying a charge on the carboxylate C15″OOH alone, whereas **1a.2** represents the same analogue bearing charges on the amine N1, the penolic C′6′OH, and the carboxylate C15″OOH. **1a.2** is not present in PKA as suggested by our previous study.[1]

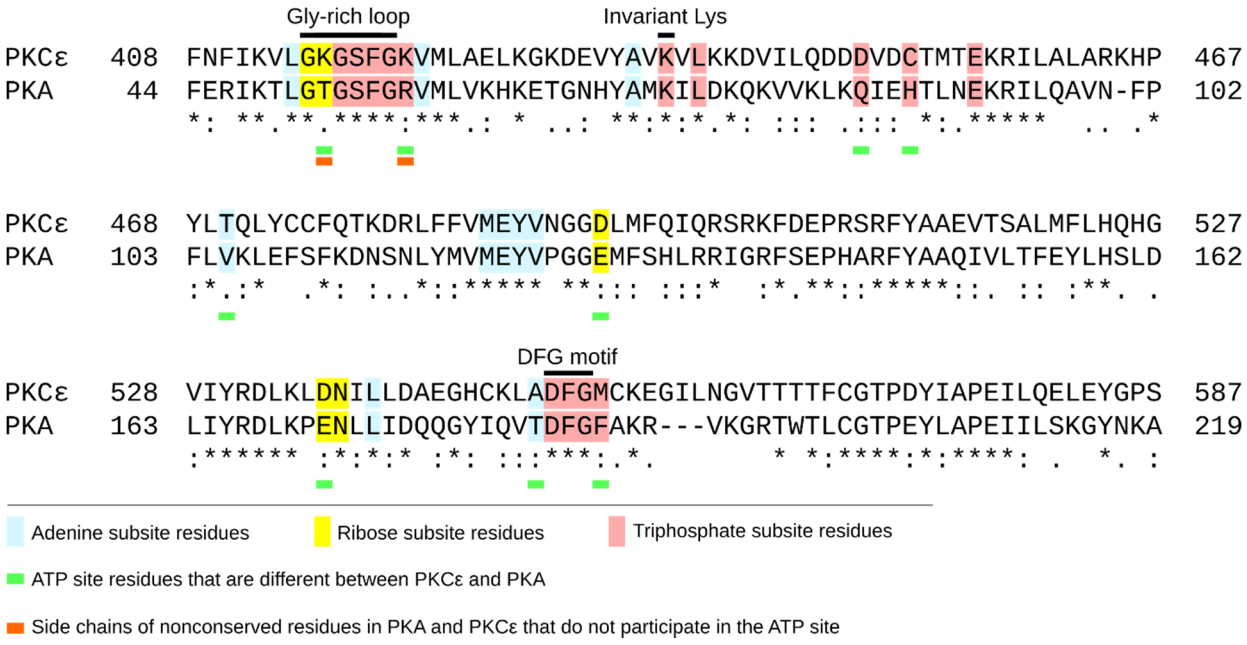

Figure S5 Sequence alignment of the ATP site residues of PKCε and PKA. Adenine, ribose, and triphosphate subsite residues are highlighted in yellow, pink, and light blue, respectively. Green bars indicate the non-identical ATP site residues in PKA and PKCε. The orange bars represent residues in PKA and PKCε contributing to the ATP site *via* backbone interactions alone. ***** – identical residue; **:** – conservative substitution; **.** – non-conservative substitution.

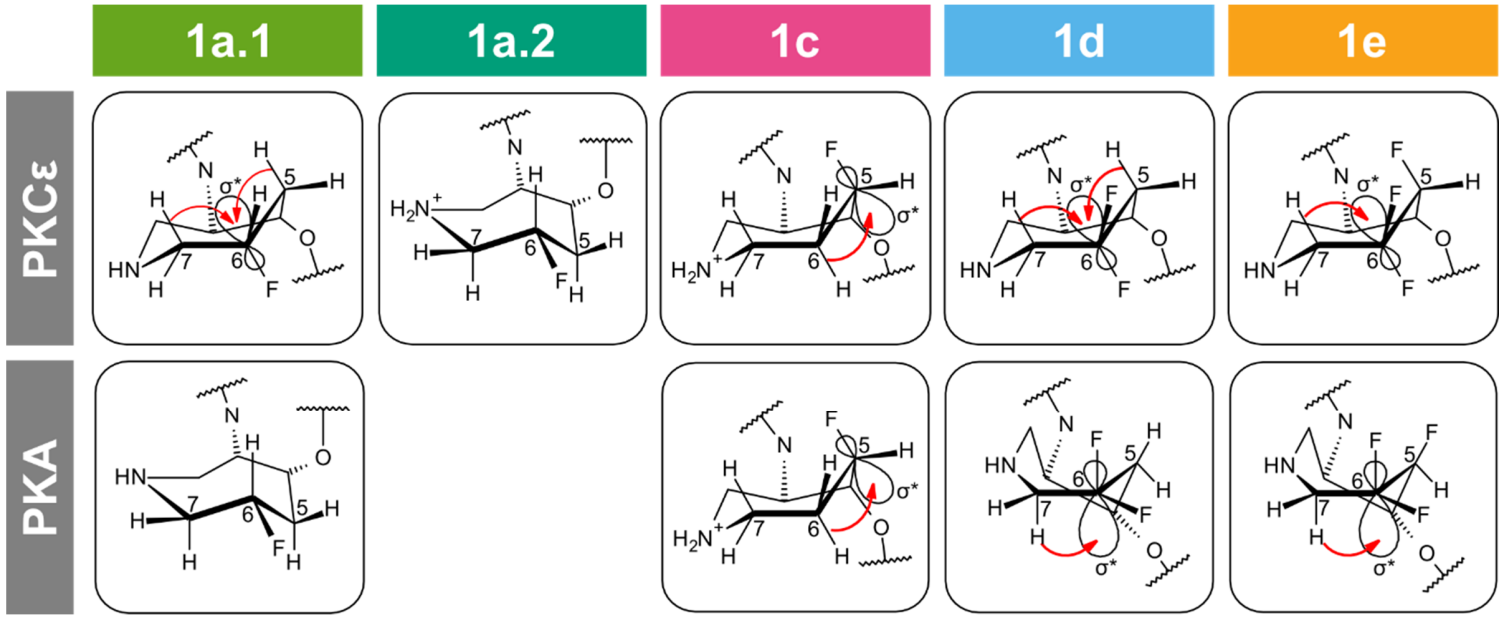

Figure S6 Hyperconjugation interactions occurring in the azepane ring of fluorinated balanol analogues. 1a.1 is species of the C6(*S*)-fluorinated analogue carrying only a charge on the carboxylate C15″OOH, whereas **1a.2** is species of the same analogue which bears charges on the amine N1, the phenolic C′6′OH, and the carboxylate C15″OOH. **1a.2** presents in PKCε but not PKA as suggested in our previous study.[1]

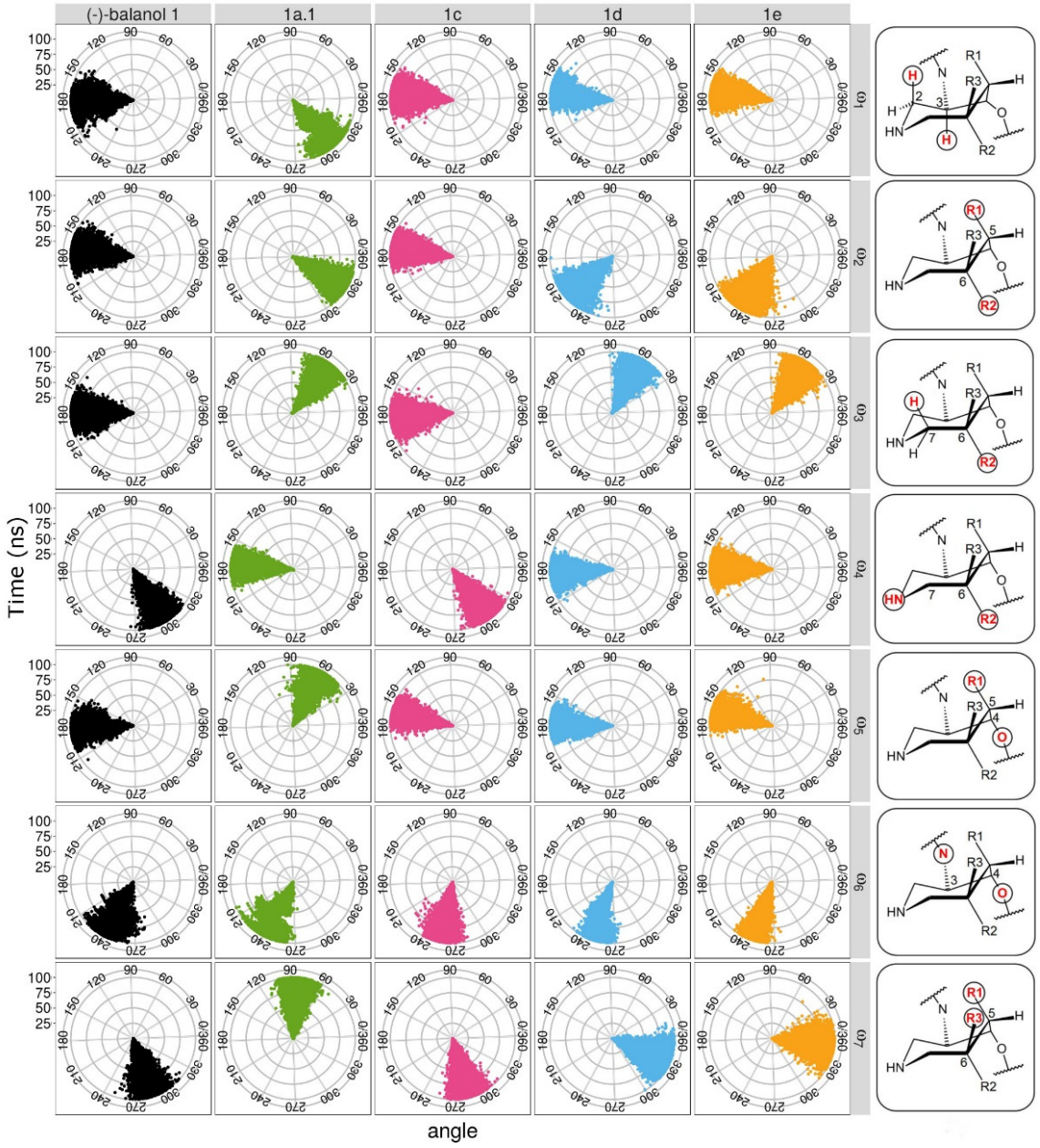

Figure S7 Polar charts of dihedral angles on the azepane ring of PKA-bound balanoids. Plots on each row monitor specific dihedral angles between the azepane ring atoms coloured red in the structures on the right panel.

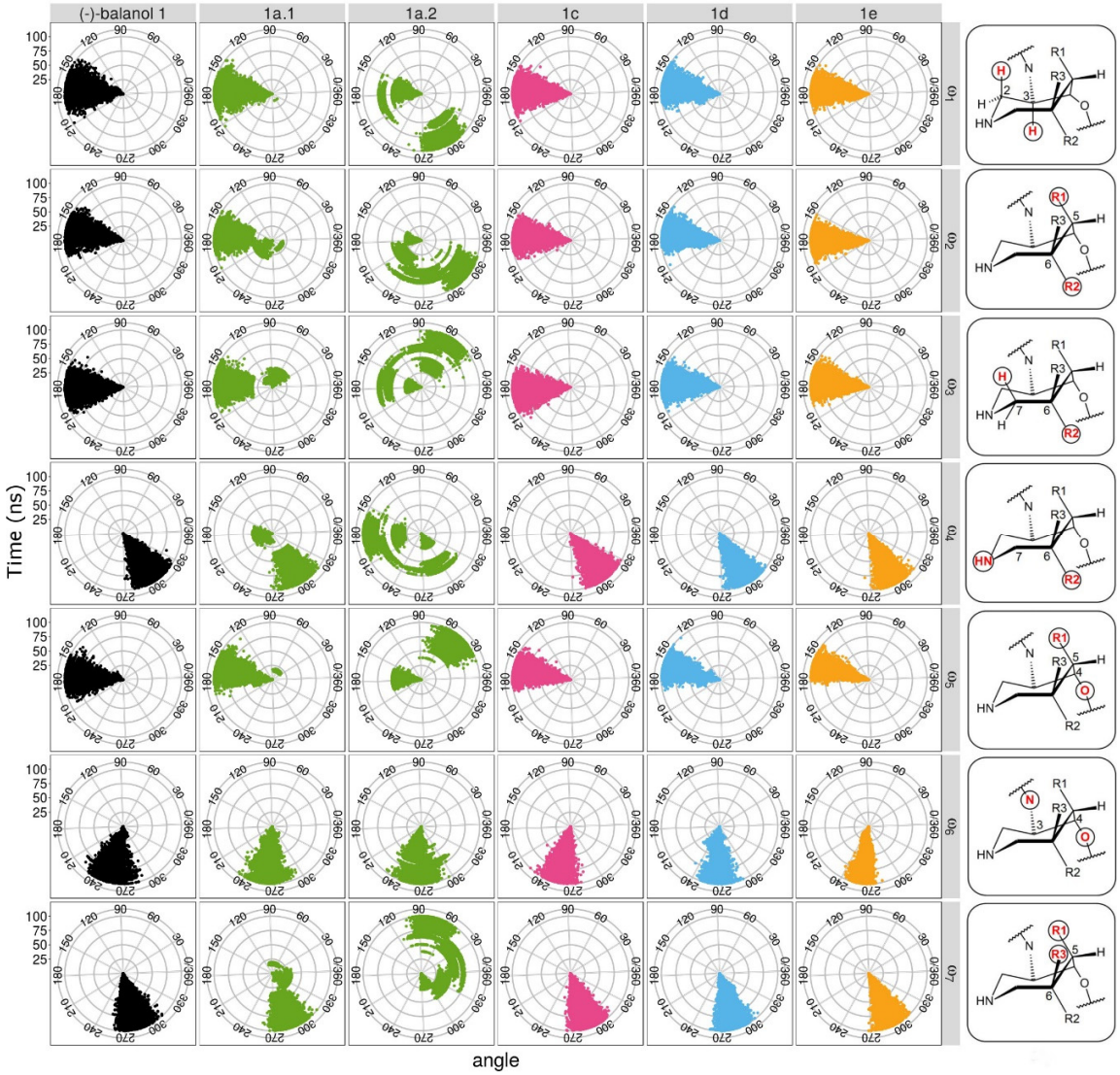

Figure S8 Polar charts of dihedral angles on the azepane ring of PKCε-bound balanoids. Plots on each row monitor specific dihedral angles between the azepane ring atoms coloured red in the structures on the right panel.

Balanoid Moiety	PKA	ΔG° Contribution (kcal.mol^{-1})							PKCε	ΔG° Contribution (kcal.mol^{-1})							
		Balanoids					Mean	SD		Balanoids						Mean	SD
	Residue	1	1a.1	1c	1d	1e			Residue	1	1a.1	1a.2	1c	1d	1e		
Benzophenone	Gly53	-4.65	-5.30	-5.06	-5.62	-6.39	-5.40	0.65	Gly417	-2.76	-4.97	-4.97	-4.58	-5.69	-5.94	-4.82	1.13
	Ser54	-4.07	-7.72	-4.40	-9.32	-8.57	-6.82	2.42	Ser418	-0.92	-7.14	-7.14	-3.66	-9.05	-7.72	-5.94	3.03
	Phe55	-5.89	-4.82	-5.84	-4.75	-5.93	-5.44	0.60	Phe419	-2.29	-5.18	-5.18	-6.62	-5.35	-5.68	-5.05	1.46
	Gly56	-2.90	-1.97	-2.65	-2.22	-2.65	-2.48	0.37	Gly420	-3.93	-1.82	-1.82	-3.49	-2.38	-1.91	-2.56	0.93
	Arg57	-3.19	-2.16	-3.39	-2.85	-2.61	-2.84	0.48	Lys421	-3.42	-1.82	-1.82	-2.60	-2.54	-2.02	-2.37	0.62
	Lys73	**-12.13**	**-8.54**	**-9.70**	**-13.76**	**-11.70**	**-11.16**	**2.06**	**Lys437**	**-18.48**	**-12.86**	**-12.86**	**-21.39**	**-13.82**	**-18.55**	**-16.33**	**3.62**
	Leu75	-2.42	-2.42	-2.77	-2.97	-2.04	-2.52	0.36	Leu439	-3.53	-2.89	-2.89	-2.70	-2.91	-3.17	-3.02	0.29
	Gln85	-0.02	-0.13	-0.02	-0.03	-0.01	-0.04	0.05	Asp449	-0.87	0.02	-0.01	-0.09	0.05	-0.25	-0.19	0.35
	His88	-0.25	-1.69	-1.44	-1.85	-0.27	-1.10	0.78	Cys452	-1.14	-1.41	-1.41	-1.45	-1.56	-1.48	-1.41	0.14
	Glu92	-7.38	-1.58	-8.06	-5.33	0.40	-4.39	3.68	Glu456	-7.80	-5.19	-5.19	-5.89	-5.25	-5.26	-5.76	1.03
	Gly187	-2.11	-1.95	-1.66	-1.69	-1.77	-1.83	0.19	Gly552	-1.07	-1.58	-1.11	-0.79	-1.16	-0.61	-1.05	0.34
Azepane	Gly51	-3.11	-2.82	-2.38	-3.45	-2.82	-2.92	0.40	Gly415	-2.24	-2.89	-2.89	-2.89	-2.83	-2.74	-2.74	0.26
	Thr52	-3.85	-3.02	-4.12	-3.59	-3.49	-3.61	0.41	Lys416	-3.42	-3.05	-3.05	-3.66	-4.01	-4.18	-3.56	0.48
	Glu128	-0.31	-0.89	-0.55	-0.45	-0.62	-0.56	0.22	Asp493	-0.10	-0.15	-0.31	-0.07	-0.29	-0.08	-0.17	0.11
	Glu171	-1.99	-3.48	-3.82	-1.72	-3.99	-3.00	1.06	Asp536	-2.39	-2.79	-3.23	-0.77	-1.07	-1.73	-2.00	0.97
	Asn172	-2.93	-1.46	-0.92	-1.07	-2.47	-1.77	0.89	Asn537	-5.18	-8.30	-8.30	-5.60	0.28	-4.83	-5.32	3.15
	Asp185	-3.14	-9.70	-2.52	-4.26	-1.09	-4.14	3.31	Asp550	-1.59	-1.71	-0.74	-2.57	-1.16	-5.30	-2.18	1.65
Benzamide	Leu50	-1.97	-2.01	-1.88	-1.97	-2.00	-1.97	0.05	Leu414	-1.69	-2.09	-2.03	-1.88	-1.79	-2.54	-2.00	0.30
	Val58	-5.07	-4.92	-4.92	-4.63	-4.91	-4.89	0.16	Val422	-5.06	-4.63	-4.63	-5.37	-4.89	-4.45	-4.84	0.34
	Ala71	-1.60	-1.61	-1.54	-1.65	-1.61	-1.60	0.04	Ala435	-1.41	-1.25	-1.40	-1.67	-1.36	-1.28	-1.40	0.15
	Val105	-1.09	-1.10	-1.28	-1.45	-1.18	-1.22	0.15	Thr470	-0.96	-0.93	-0.91	-1.13	-0.83	-0.65	-0.90	0.16
	Met121	-1.47	-1.28	-1.64	-1.79	-1.47	-1.53	0.19	Met486	-1.41	-1.39	-1.62	-1.50	-1.47	-1.30	-1.45	0.11
	Glu122	-2.67	-3.01	-1.86	-2.18	-2.65	-2.47	0.45	Glu487	-2.94	-2.98	-2.68	-3.05	-2.32	-0.39	-2.39	1.02
	Tyr123	-2.01	-2.09	-2.21	-2.17	-2.21	-2.14	0.09	Tyr488	-1.88	-1.88	-2.01	-1.94	-2.09	-0.85	-1.78	0.46
	Val124	-2.31	-2.22	-2.56	-2.29	-2.48	-2.37	0.14	Val489	-2.45	-2.53	-2.53	-2.41	-2.53	-1.08	-2.25	0.58
	Leu174	-2.64	-2.95	-3.08	-3.19	-3.06	-2.98	0.21	Leu539	-2.17	-2.49	-2.49	-3.40	-3.25	-2.68	-2.75	0.48
	Thr184	**-4.06**	**-3.70**	**-4.54**	**-4.61**	**-5.13**	**-4.41**	**0.55**	**Ala549**	**-2.37**	**-2.59**	**-2.59**	**-1.96**	**-1.74**	**-1.98**	**-2.21**	**0.36**
MMGBSA	ΔG° (kcal.mol^{-1})	-66.84	-64.95	-63.77	-58.62	-55.96			ΔG° (kcal.mol^{-1})	-67.52	-63.73	-66.93	-73.80	-46.22	-56.22		
	K_d (nM)	5.9	7.9	6.4	9.2	43			K_d (nM)	0.73	19	19	0.4	110	38		

Color scale -22 -21 -20 -19 -18 -17 -16 -15 -14 -13 -12 -11 -10 -9 -8 -7 -6 -5 -4 -3 -2 -1 0 1 kcal.mol^{-1}

Figure S9 Per-residue binding energy contributions to the affinity of balanoids to the ATP sites of PKA and PKCε. The key determinant residues, Thr184 in PKA and Ala549 in PKCε, are in bold text and highlighted in brown. The invariant Lys residues, Lys73 and Lys437 respectively in PKA and PKCε, are in bold text and highlighted in dark purple. MMGBSA binding energy as well as the experimental K_d values of balanoids bound to PKA and PKCε are in the lower panel of the figure.

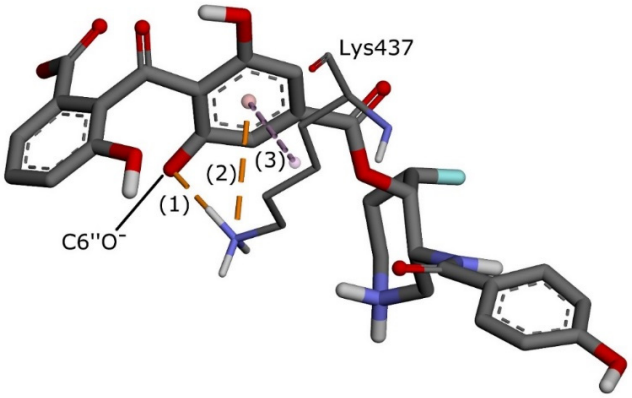

Figure S10 Interactions between the invariant Lys437 in PKCε and the phenolate C6′O$^-$ in balanoid 1c. (1) indicates H-bond and charge-charge or ion pair interactions which forms salt bridge, whereas (2) and (3) denote cation-π and alkyl-π hydrophobic interactions.

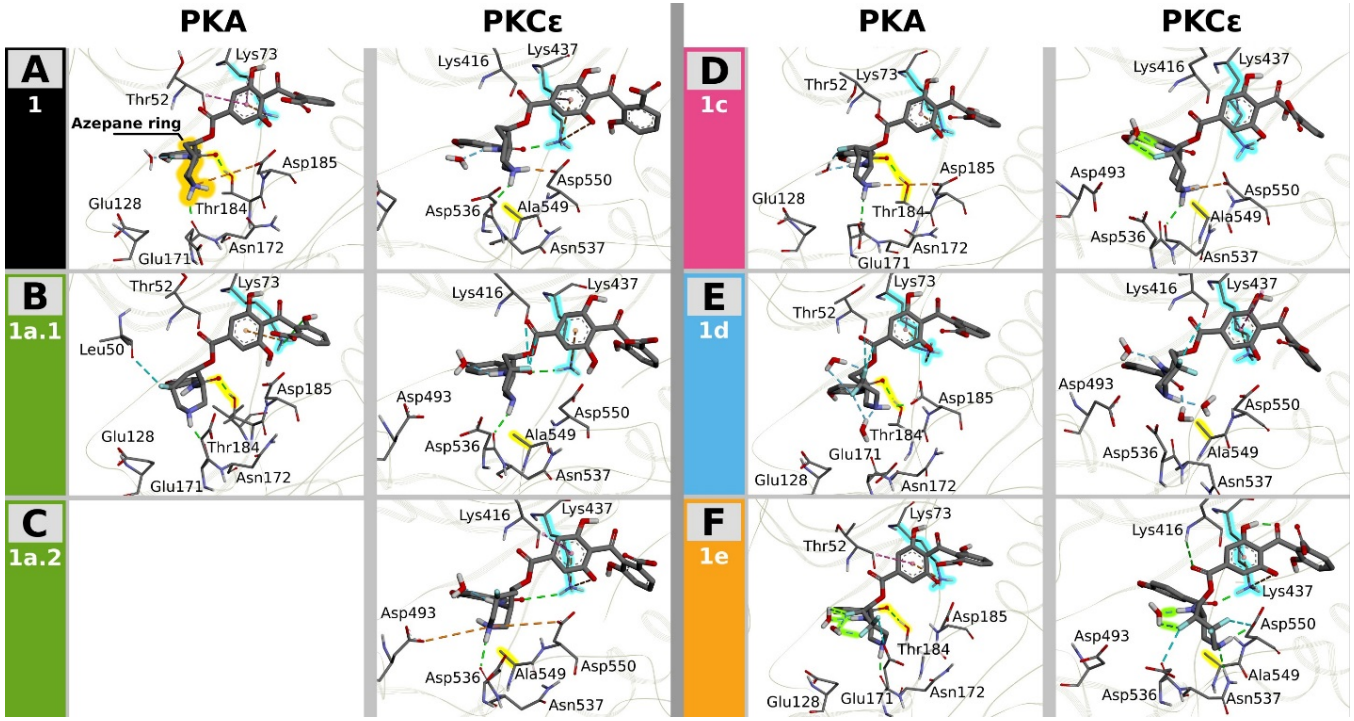

Figure S11 Interactions between balanoids and the ATP sites of PKA and PKCε which focus on the residues around the azepane ring and invariant Lys. The sub-figures depict interactions of (A) natural balanol **1**, (B) **1a.1**, (C) **1a.2**, (D) **1c**, (E) **1d**, and (F) **1e**. **1a.1** is species of the C6(*S*)-fluorinated analogue only carrying a charge on the carboxylate C15″OOH, whereas **1a.2** is species of the same analogue which bears charges on the amine N1, the phenolic C′6′OH, and the carboxylate C15″OOH. **1a.2** presents in PKCε but not PKA as suggested in our previous study.[1] The invariant Lys and the representative azepane ring are highlighted in cyan and orange, respectively. The key determinant residue (Thr184 in PKA and Ala549 in PKCε) is highlighted in yellow. Water-mediated intramolecular interactions are highlighted in green

References

(1) Hunter, L., The C-F Bond as a Conformational Tool in Organic and Biological Chemistry. *Beilstein J. Org. Chem.* **2010**, *6*, 38.

(2) Gillis, E. P.; Eastman, K. J.; Hill, M. D.; Donnelly, D. J.; Meanwell, N. A., Applications of Fluorine in Medicinal Chemistry. *J. Med. Chem.* **2015**, *58*, 8315-59.

(3) Tozer, D. J., The conformation and internal rotational barrier of benzyl fluoride. *Chem. Phys. Lett.* **1999**, *308*, 160-164.

(4) Juaristi, E.; Cuevas, G., Recent studies of the anomeric effect. *Tetrahedron Lett.* **1992**, *48*, 5019-5087.

(5) Kirsch, P., *Modern fluoroorganic chemistry: synthesis, reactivity, applications*. Wiely–VCH: Weinheim, Germany, 2004.

(6) Hardianto, A.; Yusuf, M.; Liu, F.; Ranganathan, S., Exploration of Charge States of Balanol Analogues Acting as ATP-Competitive Inhibitors in Kinases. *BMC Bioinformatics* **2017**, *18*, 572.

(7) Patel, A. R.; Ball, G.; Hunter, L.; Liu, F., Conformational regulation of substituted azepanes through selective monofluorination. *Org. Biomol. Chem.* **2013**, *11*, 3781-3785.

(8) Patel, A. R.; Hardianto, A.; Ranganathan, S.; Liu, F., Divergent response of homologous ATP sites to stereospecific ligand fluorination for selectivity enhancement. *Org. Biomol. Chem.* **2017**, *15*, 1570-1574.